Proceedings of the IASS 2024 Symposium
Redefining the Art of Structural Design
August 26-30, 2024, Zurich Switzerland
Philippe Block, Giulia Boller, Catherine DeWolf,
Jacqueline Pauli, Walter Kaufmann (eds.)

Clustering-based periodic structural optimization with variable orientations of unit cells

Yunzhen HE[1] and Yi Min XIE[1,*]

[1,*] Centre for Innovative Structures and Materials, School of Engineering, RMIT University
Melbourne 3001, Australia
mike.xie@rmit.edu.au

Abstract

In recent years, periodic structural optimization has become an effective approach to generating efficient structures that meet a variety of practical considerations, including manufacturability, transportability, replaceability, and ease of assembly. Traditional periodic structural optimization typically restricts designs to a uniform assembly configuration utilizing only one type of unit cell. This study introduces a novel clustering-based approach for periodic structural optimization, which allows variable orientations of individual unit cells. A dynamic *k*-means clustering technique is introduced to categorize all unit cells into distinct groups. Meanwhile, a heuristic approach is implemented to identify and select the most beneficial orientation configurations of the unit cells during the optimization process. Several numerical examples are presented to demonstrate the effectiveness of the proposed method. The results indicate that clustering-based oriented periodic structures can significantly outperform their traditional periodic counterparts. This study not only incorporates assembly flexibility into periodic topology optimization but also utilizes various types of unit cells, thereby further enhancing the structural performance of the periodic design.

Keywords: Topology optimization; Periodic structure; Bi-directional evolutionary structural optimization (BESO); Dynamic clustering; Oriented unit cells

1. Introduction

In recent decades, topology optimization techniques have made significant contributions to a wide range of engineering applications, e.g., advanced manufacturing [1, 2], architectural design [3-5], and civil engineering [6]. Despite their growing popularity, the optimized designs from conventional optimization techniques often feature complex geometries that pose significant manufacturing challenges. For practical applications, the optimized design requires specific adaptations, such as structural periodicity [1, 2]. This approach introduces a periodic design framework, where an individual unit cell is optimized and then replicated, creating a larger periodic structure. Specifically, periodic topology optimization can be categorized into two distinct research branches based on the size of the unit cells. For the design of microstructural materials, the unit cell, or the microstructure, is infinitely small compared to the macrostructure [7, 8]. On the other hand, this study focuses on unit cells of finite size and is primarily used for the design of large macrostructures [9, 10].

Huang and Xie initially proposed a general design framework for finite periodic optimization [9], with a primary focus on minimizing structural mean compliance. Subsequently, this approach has been extended to address other problems, including thermal conductivity [11] and natural frequency [12]. Besides the above applications, finite periodic optimization possesses significant potential in civil and architectural engineering, especially for prefabricated construction projects. Its ability to produce repetitive, standardized components fits perfectly with the modular nature of prefabricated structures.

However, most existing studies on periodic optimization have not considered the assembly flexibility of prefabricated structures. They typically adhere to one orientation configuration, yet allowing variable orientations for the unit cells can generate more efficient periodic designs [13].

Moreover, introducing more unit cell types during the optimization process is also a viable technique to improve structural performance further. Particularly in prefabricated construction projects, which usually involve assembling multiple component types, the simultaneous consideration of variable orientations for unit cells and the introduction of additional unit cell types during the form-finding process can lead to significant performance improvements. The combined benefits can be demonstrated in the following case study (Figure 1). While Figure 1b shows an optimized design maintaining a uniform orientation, Figure 1c presents a design that achieves greater efficiency by incorporating orientation flexibility. This case underscores the crucial role of selecting better orientations in periodic optimization to achieve more efficient design solutions. Moreover, as Figure 1d presents, adding a second type of unit cell can significantly improve the structural efficiency, thereby showcasing the potential of introducing more types of unit cells in the optimization process.

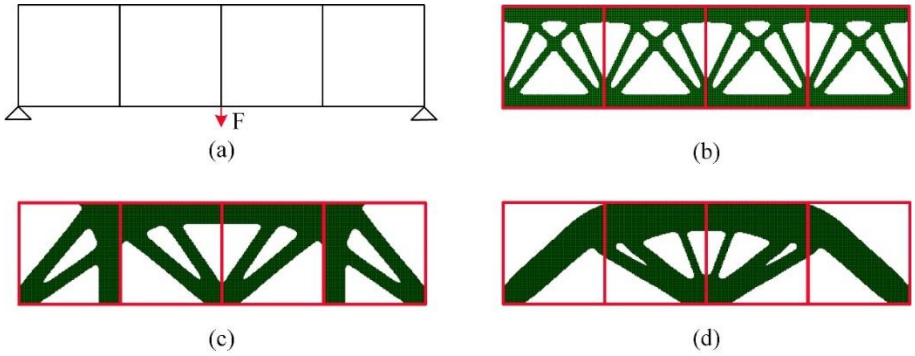

Figure 1: Different design approaches for bridges use the same material volume. (a) The loading and boundary conditions. (b) The optimized design with a uniform orientation ($C = C_0$). (c) The optimized design with oriented unit cells ($C = 0.84C_0$). (d) The oriented optimized design with two types of unit cells ($C = 0.73C_0$).

Motivated by the great potential to increase structural efficiency via orientation variability and unit cell diversity, this paper presents a clustering-based approach tailored for finite periodic structural optimization. Through numerical examples, we demonstrate that our method can obtain better outcomes. The rest of the paper is organized as follows. The topology optimization formulation for periodic design is first described in Section 2. The dynamic clustering and orientation strategies are then discussed in Section 3. Section 4 presents several numerical examples to demonstrate the effectiveness of the new approach. The main conclusions from this study are summarized in Section 5.

2. Optimization formulation and sensitivity analysis

This study presents the mean compliance minimization problem as an example to illustrate the proposed method. As shown in Figure 2, the design domain is tessellated with $m = m_1 \times m_2$ oriented unit cells where m_1 and m_2 denote the numbers of unit cells along the x and y directions, respectively. The optimization problem for the periodic structure can be described as

$$\text{Minimize: } C(x_{i,j}) = \frac{1}{2}\mathbf{U}^{\mathrm{T}}\mathbf{K}\mathbf{U} = \frac{1}{2}\sum_{i=1}^{N\times m} x_{i,j}^{p}\mathbf{u}_{i,j}^{\mathrm{T}}\mathbf{k}_{i,j}\mathbf{u}_{i,j} \tag{1}$$

$$\begin{aligned} \text{Subject to: } & V^{*} - \sum_{i}^{m}\left(\sum_{j=1}^{N} x_{i,j}v_{i,j}\right) = 0 \\ & \forall i_1, i_2 \text{ such that } i_1, i_2 \in S_k,\ x_{i_1,j} = x_{i_2,j} \\ & x_{i,j} = 1 \text{ or } x_{\min} \end{aligned} \tag{2}$$

where C is the mean structural compliance. The binary design variable $x_{i,j}$ declares the solid (1) or void ($x_{\min} = 0.001$) status of the j-th element in the i-th unit cell. N is the total number of elements within a unit cell. **U** and **K** are the global displacement vector and stiffness matrix, respectively. p is the penalty exponent [14], which is set as 3 in this paper. $\mathbf{u}_{i,j}$ is the elemental displacement vector and $\mathbf{k}_{i,j}$ is the stiffness matrix of the j-th element in the i-th unit cell. $V^* = V \times v_f$ is the target volume of the final structure. V is the total volume of the design domain, and v_f is the target volume fraction of material. $v_{i,j}$ is the volume of the j-th element in the i-th unit cell. The status of the j-th element remains the same across all unit cells that are classified as the same cluster S_k, where the set S_k includes the indices of all unit cells belonging to the k-th cluster.

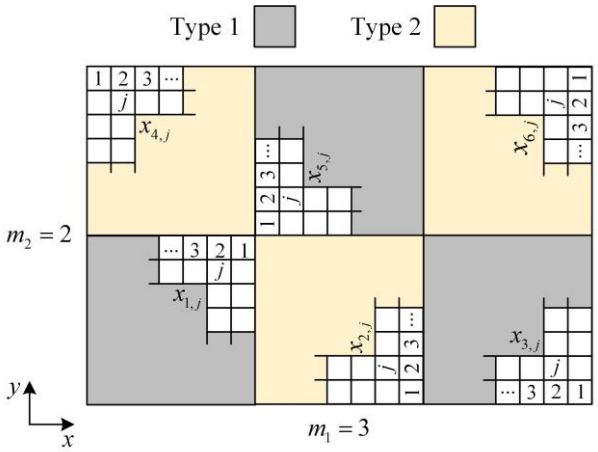

Figure 2: A 2D design domain with $m = 6$ unit cells where $m = m_1 \times m_2$. m_1 and m_2 denote the number of unit cells along the x and y direction, respectively. Here $x_{i,j}$ is the design variables where i and j denote the unit cell number and element number within the unit cell, respectively.

In the BESO method, the design variables are updated iteratively according to the relative ranking of the sensitivities. By using the adjoint method [15], the gradient of the objective function C with regard to the design variable $x_{i,j}$ can be calculated as

$$\frac{\partial C}{\partial x_{i,j}} = -\frac{1}{2} p x_{i,j}^{p-1} \mathbf{u}_{i,j}^T \mathbf{k}_{i,j} \mathbf{u}_{i,j} \tag{3}$$

The sensitivity of element j within unit cell i is defined as

$$\alpha_{i,j} = -\frac{1}{p v_{i,j}} \frac{\partial C}{\partial x_{i,j}} \tag{4}$$

To avoid checkerboard pattern and mesh-dependency issues, the following filtering scheme is adopted to process the raw sensitivity for each individual element [16].

$$\tilde{\alpha}_{i,j} = \frac{\sum_{k=1}^{N} w_{(i,j)k} \alpha_k}{\sum_{k=1}^{N} w_{(i,j)k}} \tag{5}$$

$$w_{(i,j)k} = \max\left(0, r_f - d_{(i,j)k}\right) \tag{6}$$

where N is the total number of elements in the circular sub-domain of the filter scheme. $w_{(i,j)k}$ is the linear weight factor, r_f the filter radius, and $d_{(i,j)k}$ is the distance between the centers of elements (i, j) and k. To stabilize the optimization process and ensure the convergence of solutions, the smoothed sensitivity of the current iteration is adjusted by averaging its historical values as follows [17]

$$\bar{\alpha}_{i,j} = \frac{\tilde{\alpha}_{i,j}^{(n)} + \bar{\alpha}_{i,j}^{(n-1)}}{2}, \ (n \geq 2) \tag{7}$$

In this study, the historical values of sensitivity numbers play a crucial role in determining the orientations of unit cells and clustering them into distinct groups. The clustering and orientation strategies will be discussed in the following sections.

3. Methodology

3.1. Dynamic clustering technique

The proposed approach uses a dynamic *k*-means clustering technique to classify all unit cells into different clusters based on their structural efficiency. Moreover, the inefficient unit cells can be gradually removed during the optimization process. A minimum volume fraction $v_{\mathrm{f\,min}}$ is set to remove unit cells with volume fractions below this threshold. These unit cells are then manually classified as void unit cells S_0 in the subsequent clustering process. The details of the dynamic clustering technique are presented in Algorithm 1 as follows:

Step 1: For every *g*-th iteration, update the number of clusters N^C using Eq. (8).

$$N^C = \left\lfloor (k-m) \times \left(\frac{1-v_{\mathrm{c}}}{1-v_{\mathrm{f}}} \right)^{\eta} + m \right\rfloor \tag{8}$$

where k represents the target number of clusters, v_{c} is the current volume fraction, and v_{f} is the final volume fraction. η is used to control the rate of change in the number of clusters. Once the objective volume fraction is reached, the number of clusters will be maintained at the target value k.

Step 2: Perform finite element analysis and calculate the elemental sensitivity according to Eq. (7).

Step 3: Calculate the number of void unit cells $|S_0|$ in the current iteration based on the minimum volume fraction threshold $v_{\mathrm{f\,min}}$.

Step 4: Calculate the sample point $\bar{\mathbf{s}}_i$ for each unit cell. The clustering sample point for each unit cell $\bar{\mathbf{s}}_i$ comprises two key metrics: the mean $\bar{\mathbf{x}}_i$ and the variance $\bar{\mathbf{y}}_i$ of the sensitivities across all its elements.

Step 5: Rank all unit cells and update the void cluster S_0 based on the mean sensitivity $\bar{\mathbf{x}}_i$ of each unit cell.

Step 6: The *k*-means method is employed to cluster the sample set $\bar{\mathbf{S}} = \left\{ \forall \bar{\mathbf{s}}_i \,|\, i \notin S_0 \right\}$, excluding void unit cells.

3.2. Determining the orientations of unit cells

In finite periodic optimization, a straightforward way to compute the sensitivity of the *j*-th element within the representative unit cell (RUC) is to average the sensitivities of the corresponding *j*-th elements across all unit cells in the same cluster [9]. This can be executed as follows

$$\alpha_{S_k,j} = \frac{\sum_{i \in S_k} \alpha_{i,j}}{|S_k|} \tag{9}$$

where $\alpha_{Sk,j}$ is the sensitivity number of the *j*-th element in the *k*-th RUC. As shown in Figure 2, the RUC sensitivities $\alpha_{Sk,j}$ may vary according to the orientation of the constituent unit cells within each cluster.

Thus, identifying more efficient configurations could lead to significantly better local optima for the optimization problem.

A practical approach to achieving a better orientation configuration is to determine the orientation of each unit cell by associating the relatively higher-ranked elements within these unit cells. As shown in Figure 3, we may divide each unit cell into four quadrants and then calculate the total sensitivities of all elements within each quadrant. Initially, the quadrant with the highest sensitivity value is identified and assigned the number 1 (Figure 3). Subsequently, the adjacent quadrant (excluding diagonals) with the next highest sensitivity value is marked with the number 2 (Figure 3). The remaining two quadrants are then labeled with the number 0. Consequently, each unit cell is assigned an orientation sequence code, represented as O_i, which in turn determines the orientation of the unit cell (Figure 3). All these orientation sequence codes together form the orientation configuration of the macrostructure, which is denoted as $\mathbf{O} = [O_1,\ldots,O_i, \ldots,O_m]$.

To determine the sensitivities of the RUC for each type, one can choose a reference unit cell with a specific sequence code as the benchmark. Subsequently, all other unit cells within the same type are re-oriented to match the benchmark sequence code. Figure 4a provides several examples demonstrating the method for calculating the RUC sensitivities of each cluster according to Eq. (9). For instance, in Figure 4a, sequence code 1200 is chosen for the reference unit cell. If unit cell one also has the sequence code 1200, then its orientation aligns with that of the reference unit cell. On the other hand, if the sequence code for unit cell two is 0012, then its orientation is adjusted to mirror the reference unit cell. Similarly, unit cell three is required to be rotated anti-clockwise by 90 degrees. Once the RUC design is updated, the design variables of elements in each unit cell are reassigned based on its orientation sequence code and corresponding RUC design (Figure 4b).

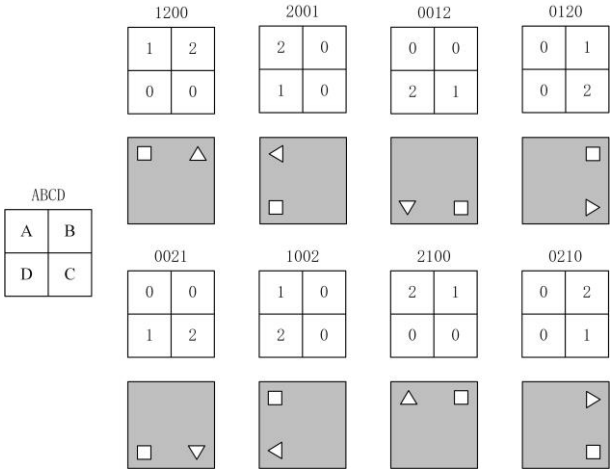

Figure 3: Illustration of possible orientations of 2D square unit cells with corresponding sequence codes.

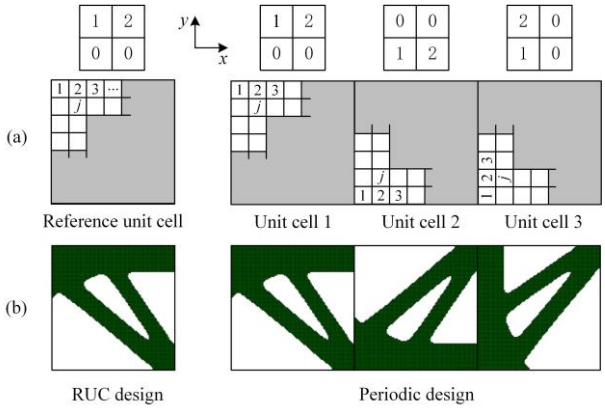

Figure 4: Illustration of how to calculate the RUC sensitivities and update the periodic design.

3.3. The element update scheme

In the conventional periodic optimization, both the sensitivities and design variables are updated within the RUC domain [9]. This study does not retain historical sensitivities within the RUC due to the implementation of a dynamic clustering technique. This technique allows for the number of clusters and their respective unit cells to vary during optimization. Therefore, the historical sensitivities are individually recorded for each unit cell. The update of the RUC sensitivities can be outlined in Algorithm 2 as follows:

Step 1. Calculate the raw RUC sensitivities of each cluster $\alpha_{S_k,j}^n$ according to Eq. (9).

Step 2. Obtain the smoothed RUC sensitivities $\tilde{\alpha}_{S_k,j}^n$ of each cluster according to the filter scheme in Eqs. (5) and (6).

Step 3. The smoothed RUC sensitivities of the current iteration $\tilde{\alpha}_{S_k,j}^n$ ($n \geq 2$) are averaged with the historical sensitivities of each individual unit cell $\bar{\alpha}_{i,j}^{(n-1)}$. This can be achieved by slightly modifying Eq. (7) as $\bar{\alpha}_{i,j}^n = \left(\tilde{\alpha}_{S_k,j}^n + \bar{\alpha}_{i,j}^{(n-1)}\right)/2,\ \left(i = 1,2,\cdots,m\right)$. It is important to note that the smoothed sensitivities of the RUCs $\tilde{\alpha}_{S_k,j}^n$ are oriented based on the orientation sequence code obtained from the orientation technique outlined in Section 3.2.

Step 4. Update the RUC sensitivities according to the averaged RUC sensitivities. This step can be realized by making a minor adjustment to Eq. (9) as $\hat{\alpha}_{S_k,j} = \sum_{i \in S_k} \bar{\alpha}_{i,j}^n / \left|S_k\right|$.

Step 5. Obtain the smoothed sensitivity $\tilde{\tilde{\alpha}}_{S_k,j}$ for the updated RUC sensitivities $\hat{\alpha}_{S_k,j}$ by applying the filter scheme according to Eqs. (5) and (6).

After obtaining the final RUC sensitivities $\tilde{\tilde{\alpha}}_{S_k,j}$, the target volume $V^{(n)}$ of material for the next iteration needs to be determined to update the design variables:

$$V^{(n)} = \max\left\{V^*, V^{(n-1)}\left(1-\delta\right)\right\} \tag{10}$$

where δ is the evolutionary ratio. During the optimization process, the material volume gradually decreases to the target value V^*. In each iteration, the element update involves setting a sensitivity threshold to achieve the target volume. The solid elements with sensitivities lower than the threshold are removed from the RUC domain. In contrast, the removed elements with sensitivities higher than the threshold are readmitted to the RUC domain. The sensitivity threshold is determined by a bisection method, as outlined in Table 1.

Table 1: Pseudocode of the bisection method

Input: RUC sensitivities $\tilde{\tilde{\alpha}}_{S_k,j}$, design variables $x_{i,j}$, target volume $V^{(n)}$

$th_{\text{low}} = \min(\tilde{\tilde{\alpha}}_{S_k,j}),\ th_{\text{high}} = \max(\tilde{\tilde{\alpha}}_{S_k,j})$
While $\left(th_{\text{high}} - th_{\text{low}}\right)/th_{\text{high}} > 10\text{e-}6$ **do**
    $th = \left(th_{\text{high}} - th_{\text{low}}\right)/2$
    for each $\tilde{\tilde{\alpha}}_{S_k,j}$ **do**
        if $\tilde{\tilde{\alpha}}_{S_k,j} > th$: $\forall x_{i,j} = 1,\ i \in S_k$ # Reassign design variables in unit cells
        else: $\forall x_{i,j} = x_{\min},\ i \in S_k \bigcup S_0$
    end
    if $\sum_i^m \left(\sum_j^N x_{i,j} v_{i,j}\right) - V^{(n)} > 0$: $th_{\text{low}} = th$
    else: $th_{\text{high}} = th$
end

Output: The updated design variables $\hat{x}_{i,j}$

3.4. Numerical implementation

The numerical implementation procedure of the clustering-based approach is described as follows.

Step 1. Discretize the design domain with a finite element mesh and assign initial design variables (1 or $x_{\min}$) to elements to construct the initial design.

Step 2. Perform FEA on the current design to obtain the raw elemental sensitivities $\alpha_{i,j}^{n}$ and the mean compliance C_n.

Step 3. For every *g*-th iteration, classify unit cells into different types S_k using Algorithm 1.

Step 4. Determine the current orientation configuration $\mathbf{O}^n$ using the technique from Section 3.2.

Step 5. Compare the new configuration $\mathbf{O}^n$ with the previous configuration $\mathbf{O}^{(n-1)}$. If $\mathbf{O}^n = \mathbf{O}^{(n-1)} \Leftrightarrow \forall i \in \{1,2,\cdots,m\}$, $O_i^n = O_i^{(n-1)}$, set the target volume $V^{(n)}$ using Eq. (10). Otherwise, maintain the previous volume as $V^{(n-1)}$.

Step 6. Update RUC sensitivities based on the new orientation $\mathbf{O}^n$ using Algorithm 2.

Step 7. Update elements to construct a new design for the next FEA using the bisection method in Table 1. If $\mathbf{O}^n = \mathbf{O}^{(n-1)}$, move to 0. Otherwise, proceed to Step 8.

Step 8. Perform FEA on the new design and obtain the mean compliance value $\hat{C}_n$. If $\hat{C}_n \le C_n$, go to 0. If $\hat{C}_n > C_n$, replace the current configuration with the previous configuration as $\mathbf{O}^n \leftarrow \mathbf{O}^{(n-1)}$ and return to Step 5.

Repeat Step 2 to Step 8 until the following convergence criterion is satisfied. The convergence criterion is applied once the final target volume V^* is achieved. Here, *n* denotes the current iteration number, τ represents the tolerance set at 0.001 for this study, and *Z*, an integer, is fixed at 5, indicating that the change in mean compliance over the last ten iterations is sufficiently small.

$$\frac{\left|\sum_{i=1}^{Z}\left(C_{n-i+1}-C_{n-Z-i+1}\right)\right|}{\sum_{i=1}^{Z}C_{n-i+1}} \le \tau \tag{11}$$

In the proposed approach, the mean compliance value is used to evaluate the competitiveness of the newly obtained configuration. When consecutive configurations differ during optimization, the material volume remains constant to facilitate an accurate comparison of orientation efficiencies. The configuration yielding a lower mean compliance value is then selected for the subsequent optimization iteration. This approach allows stable changes in the objective function and leads to a stable convergence.

4. Numerical examples

4.1. Two-dimensional beam

The first example considered here is a two-dimensional beam (Figure 5). Due to symmetry, only half of the model is used for optimization. The half-design domain is divided by 8 × 4 unit cells, with each meshed into 100 × 100 plane stress elements. Figure 5a shows the loading and boundary conditions of the optimization problem. The concentrated force $F = 1$ is applied at the bottom middle of the beam. In this example, the target volume fraction and the filter radius for all cases are set to 50% and 5, respectively. The evolutionary ratio δ is 1%.

Conventional periodic optimization is first demonstrated. Figure 5b shows the optimized design using one type of unit cell with a uniform orientation. This approach results in uniform volume fractions across all unit cells, which could lead to inefficient material distribution in areas of the structure with lower strain energy density. Figure 5c, Figure 5d, and Figure 5e present the optimized designs with different

numbers of clusters. In all cases, $v_{f\,min}$ is set to be 0. The mean compliances of Figure 5c, Figure 5d, and Figure 5e are 21%, 25%, and 38% lower than that of Figure 5b. The results of the three cases show that the proposed approach can not only identify more efficient unit cell orientations but achieve more efficient material distribution by incorporating more types of unit cells.

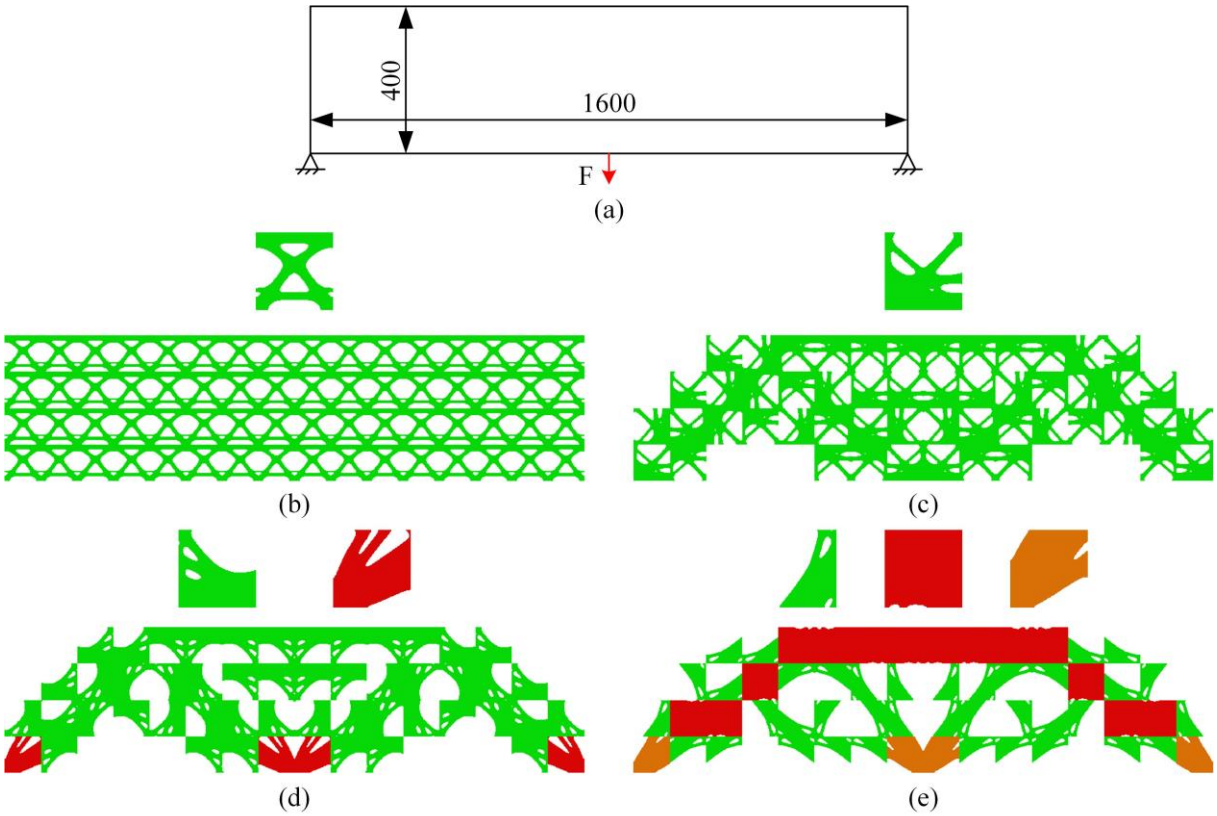

Figure 5: Example of the two-dimensional beam. (a) Loading and boundary conditions. (b) Optimized design with one unit cell type and uniform orientation (C = 60.8). Optimized designs featuring (c) one, (d) two, and (e) three types of unit cells, with mean compliance values C of 46.6, 45.8, and 37.6, respectively.

4.1. Three-dimensional cantilever beam

The proposed orientation technique in Section 3.2 can be easily extended to three-dimensional periodic optimization. For three-dimensional problems, we consider that the macro design domain is divided into multiple cubic unit cells. Similar to the square unit cell, we can divide the cubic unit cell into eight octants and then calculate the total sensitivities of all elements within each octant to determine the orientation sequence code. We can initially identify the octant with the highest sensitivity value and label it as number 1. Next, from the three adjacent face neighboring octants, we select the one with the highest sensitivity and label it as number 2. Subsequently, among the remaining two face neighboring octants, we identify the one with the highest sensitivity and label it as number 3. Lastly, all other octants are labeled with the number 0. Consequently, each cubic unit cell is assigned an orientation sequence code with eight numbers.

To illustrate the above orientation technique, we consider a three-dimensional cantilever beam with loading and boundary conditions detailed in Figure 6a. A concentrated force F = 1 is applied at the centroid of the free end. Due to symmetry, only a quarter of the model is optimized. This quarter model is divided into 60×8×4 unit cells, each further meshed into 5 × 5 × 5 hexahedral elements. The target volume fraction and the filter radius are set at v_f = 20% and r_f = 1.5, respectively. In this example, the dynamic cluster technique is applied every ten iterations, and $v_{f\,min}$ = 10%. The evolutionary ratio δ is 2%. Figure 6b, Figure 6c, and Figure 6d illustrate optimized designs with one, two, and three types of unit cells. It is evident that using more clusters in the optimization results in lower compliance values. In practice, the optimal number of clusters can be identified using the "Elbow Method." This technique

determines the optimal number of clusters by identifying a knee point on the curve plotting the objective against the number of clusters.

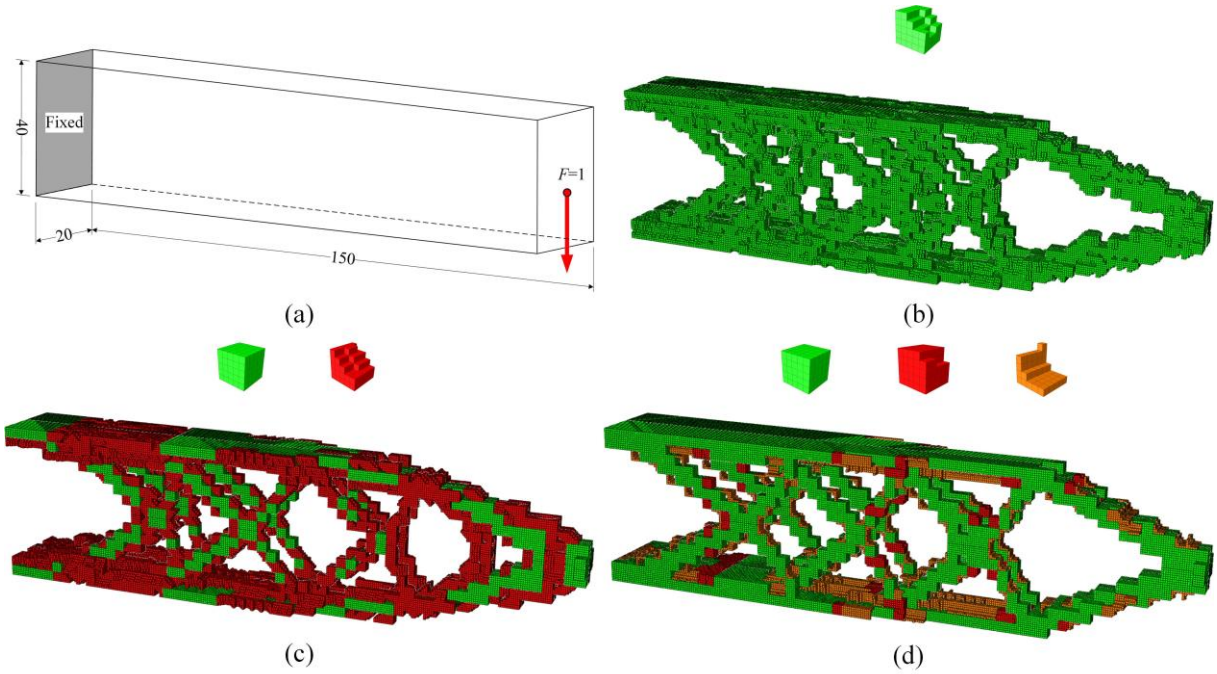

Figure 6: Example of the three-dimensional cantilever beam. (a) Loading and boundary conditions. Optimized designs featuring (b) one, (c) two, and (d) three types of unit cells, with mean compliance values C of 8.7, 7.8, and 6.6, respectively.

4. Conclusions

In this paper, we have developed a clustering-based approach for periodic structural optimization. It features an orientation technique to select more efficient orientations for unit cells during the optimization process. We propose a dynamic k-means clustering technique to eliminate less efficient unit cells and incorporate multiple unit cell types into the optimized design. The effectiveness of this approach is demonstrated through several numerical examples in the context of compliance minimization. The proposed orientation technique has proven to be effective in finding better orientation configurations with an acceptable increase in computational costs. This is particularly useful when finding the optimal unit cell orientations through brute force computation becomes impractical for structures with numerous unit cells. Moreover, the structural performance of the optimized design can be further improved as more types of unit cells are included. Therefore, in practical applications, designers can determine the number of clusters based on the trade-off between performance improvement and increased manufacturing costs.

Acknowledgements

This work is supported by the China Scholarship Council (201808430204) and the Australian Research Council (FL190100014).

References

[1] Y. He, Z. L. Zhao, K. Cai, J. Kirby, Y. Xiong, and Y. M. Xie, "A thinning algorithm based approach to controlling structural complexity in topology optimization," *Finite Elements in Analysis and Design*, vol. 207, p. 103779, 2022.

[2] Y. He, Z. L. Zhao, X. Lin, and Y. M. Xie, "A hole-filling based approach to controlling structural complexity in topology optimization," *Computer Methods in Applied Mechanics and Engineering*, vol. 416, p. 116391, 2023.

[3] Y. He, K. Cai, Z. L. Zhao, and Y. M. Xie, "Stochastic approaches to generating diverse and competitive structural designs in topology optimization," *Finite Elements in Analysis and Design*, vol. 173, p. 103399, 2020.
[4] K. Yang, Z. L. Zhao, Y. He, S. Zhou, Q. Zhou, W. Huang, and Y. M. Xie, "Simple and effective strategies for achieving diverse and competitive structural designs," *Extreme Mechanics Letters*, vol. 30, p. 100481, 2019.
[5] Y. M. Xie, K. Yang, Y. He, Z. L. Zhao, and K. Cai, "How to obtain diverse and efficient structural designs through topology optimization," in *Proceedings of IASS Annual Symposia*, 2019, vol. 2019, no. 17: International Association for Shell and Spatial Structures (IASS), pp. 1977–1984.
[6] J. Ma, Y. He, Z. L. Zhao, and Y. M. Xie, "Topology optimization of ribbed slabs and shells," *Engineering Structures*, vol. 277, p. 115454, 2023.
[7] J. Wu, O. Sigmund, and J. P. Groen, "Topology optimization of multi-scale structures: a review," *Structural and Multidisciplinary Optimization*, vol. 63, pp. 1455–1480, 2021.
[8] O. Sigmund, "Materials with prescribed constitutive parameters: An inverse homogenization problem," *International Journal of Solids and Structures*, vol. 31, pp. 2313–2329, 1994.
[9] X. Huang and Y. M. Xie, "Optimal design of periodic structures using evolutionary topology optimization," *Structural and Multidisciplinary Optimization*, vol. 36, pp. 597–606, 2008.
[10] Y. M. Xie, Z. H. Zuo, X. Huang, and J. H. Rong, "Convergence of topological patterns of optimal periodic structures under multiple scales," *Structural and Multidisciplinary Optimization*, vol. 46, pp. 41–50, 2012.
[11] Y. Chen, S. Zhou, and Q. Li, "Multiobjective topology optimization for finite periodic structures," *Computers & Structures*, vol. 88, pp. 806–811, 2010.
[12] Z. H. Zuo, Y. M. Xie, and X. Huang, "Optimal topological design of periodic structures for natural frequencies," *Journal of Structural Engineering*, vol. 137, pp. 1229–1240, 2011.
[13] S. Thomas, Q. Li, and G. Steven, "Finite periodic topology optimization with oriented unit-cells," *Structural and Multidisciplinary Optimization*, vol. 64, pp. 1765–1779, 2021.
[14] M. P. Bendsøe and O. Sigmund, *Topology Optimization: Theory, Methods, and Applications*. Springer, 2004.
[15] X. Huang and Y. M. Xie, *Evolutionary Topology Optimization of Continuum Structures: Methods and Applications*. John Wiley & Sons, 2010.
[16] O. Sigmund and J. Petersson, "Numerical instabilities in topology optimization: a survey on procedures dealing with checkerboards, mesh-dependencies and local minima," *Structural optimization*, vol. 16, pp. 68–75, 1998.
[17] X. Huang and Y. M. Xie, "Convergent and mesh-independent solutions for the bi-directional evolutionary structural optimization method," *Finite Elements in Analysis and Design*, vol. 43, pp. 1039–1049, 2007.